Cell Reports
Article

OPEN ACCESS
CellPress

Role of Mitochondrial Complex IV in Age-Dependent Obesity

Ines Soro-Arnaiz,[1,13] Qilong Oscar Yang Li,[1,13] Mar Torres-Capelli,[1] Florinda Meléndez-Rodríguez,[1] Sónia Veiga,[3,4,5] Koen Veys,[10,11] David Sebastian,[3,4,5] Ainara Elorza,[1] Daniel Tello,[1] Pablo Hernansanz-Agustín,[2] Sara Cogliati,[9] Jose Maria Moreno-Navarrete,[7] Eduardo Balsa,[1,12] Esther Fuertes,[1] Eduardo Romanos,[6] Antonio Martínez-Ruiz,[2] Jose Antonio Enriquez,[9] Jose Manuel Fernandez-Real,[7] Antonio Zorzano,[3,4,5] Katrien De Bock,[8] and Julián Aragonés[1,14,*]

[1]Research Unit, Hospital of Santa Cristina, Research Institute Princesa (IP), Autonomous University of Madrid, Madrid 28009, Spain
[2]Immunology Department, Hospital of La Princesa, Research Institute Princesa (IP), Autonomous University of Madrid, Madrid 28009, Spain
[3]Institute for Research in Biomedicine (IRB, Barcelona), Barcelona 08028, Spain
[4]Department of Biochemistry and Molecular Biology, University of Barcelona, Barcelona 08028, Spain
[5]CIBER of Diabetes and Metabolic Diseases (CIBERDEM), Carlos III Health Institute, Barcelona 08036, Spain
[6]Phenotyping Unit, IIS Aragón, Zaragoza 50013, Spain
[7]Department of Diabetes, Endocrinology and Nutrition, CIBEROBN Fisiopatología de la Obesidad y Nutrición, Institut d'Investigació Biomédica of Girona, Girona 17007, Spain
[8]Health Sciences and Technology Department, Laboratory of Exercise and Health, Swiss Federal Institute of Technology (ETH), Zurich 8603, Switzerland
[9]Centro Nacional de Investigaciónes Cardiovasculares (CNIC) Carlos III, Madrid 28029, Spain
[10]Laboratory of Angiogenesis and Vascular Metabolism, Vesalius Research Center, VIB, Leuven 3000, Belgium
[11]Laboratory of Angiogenesis and Vascular Metabolism, Vesalius Research Center, Department of Oncology, University of Leuven, Leuven 3000, Belgium
[12]Present address: Department of Cancer Biology, Dana-Farber Cancer Institute, Boston, MA 02115, USA
[13]Co-first author
[14]Lead Contact
*Correspondence: jaragones.hlpr@salud.madrid.org
http://dx.doi.org/10.1016/j.celrep.2016.08.041

SUMMARY

Aging is associated with progressive white adipose tissue (WAT) enlargement initiated early in life, but the molecular mechanisms involved remain unknown. Here we show that mitochondrial complex IV (CIV) activity and assembly are already repressed in white adipocytes of middle-aged mice and involve a HIF1A-dependent decline of essential CIV components such as COX5B. At the molecular level, HIF1A binds to the *Cox5b* proximal promoter and represses its expression. Silencing of *Cox5b* decreased fatty acid oxidation and promoted intracellular lipid accumulation. Moreover, local in vivo *Cox5b* silencing in WAT of young mice increased the size of adipocytes, whereas restoration of COX5B expression in aging mice counteracted adipocyte enlargement. An age-dependent reduction in *COX5B* gene expression was also found in human visceral adipose tissue. Collectively, our findings establish a pivotal role for CIV dysfunction in progressive white adipocyte enlargement during aging, which can be restored to alleviate age-dependent WAT expansion.

INTRODUCTION

With a steadily increasing incidence, obesity has become the leading medical disorder of the 21st Century. In particular, the middle-aged population appears to be prone to obesity (Ng et al., 2014; Ogden et al., 2013; van Harmelen et al., 2003). Although the reasons for this remain largely enigmatic, several factors are strongly implicated in the development of obesity, such as sedentary lifestyle and poor dietary habits. Genetic factors have also been suggested to control age-dependent obesity. For example, hypothalamic pro-opiomelanocortin neurons, which are involved in the regulation of food intake, are progressively silenced during aging (Yang et al., 2012). Most of the knowledge on fat development stems from experimental studies in which white adipose tissue (WAT) expansion occurs rapidly upon high-fat diet (HFD) feeding. The mechanisms involved in progressive WAT expansion during aging, however, remain mostly unidentified. Because obesity at a later age predisposes to life-threatening conditions such as insulin resistance, type 2 diabetes, and cardiovascular disease, understanding the causal molecular mechanisms of age-related obesity may provide a strategy for treating these disorders.

One of the hallmarks of aging is the functional dysregulation of mitochondria (López-Otín et al., 2013), which constitute the central metabolic hub in many cell types and are the gateway to aerobic metabolism. Mitochondrial oxidative phosphorylation is governed by the electron transport chain (ETC). Oxygen is the

final electron acceptor in the ETC, and cytochrome *c* oxidase (complex IV [CIV]), the terminal enzyme of the ETC, reduces it to H_2O after which energy is produced in the form of ATP by the action of ATP synthase (Saraste, 1999). In mature white adipocytes, mitochondria have a central role in many processes, such as ensuring energy generation through fatty acid β-oxidation in the mitochondrial matrix (Kusminski and Scherer, 2012; Villarroya et al., 2009). Aside from ATP production, mitochondria generate the necessary metabolic intermediates for lipid synthesis, thereby determining lipogenic potential (Kusminski and Scherer, 2012). Moreover, mitochondrial activity in WAT is associated with the release of several adipokines, including adiponectin (Kim et al., 2007; Koh et al., 2007; Kusminski and Scherer, 2012).

Aging has also been associated with increased adiposity early in the lives of mice and humans (Gargiulo et al., 2014; Kuk et al., 2009). However, it is unclear whether mitochondrial dysfunction in WAT contributes to age-related adipocyte enlargement and whether it can be restored to counteract age-dependent WAT expansion. Here we report that adipocytes of early middle-aged mice already exhibit mitochondrial dysfunction, which is largely associated with a decline of mitochondrial CIV activity and assembly. This decline in CIV activity involves a hypoxia-inducible factor 1A (HIF1A)-dependent reduction of CIV components, including cytochrome c oxidase subunit Vb (*Cox5b*). Silencing of *Cox5b* is sufficient to promote a global decline of CIV assembly, as well as decreased fat oxidation, and contributes to adipocyte enlargement during aging. Conversely, in vivo restoration of COX5B expression counteracts age-dependent white adipocyte enlargement. Collectively, our findings highlight the potential of targeting mitochondrial CIV to reverse adipocyte expansion during aging.

RESULTS

Selective Reduction of White Adipocyte Mitochondrial CIV Activity during Age-Dependent Obesity

During aging, mouse body weight progressively increased from 31.7 ± 1.2 g (in 3- to 5-month-old mice) to 43.3 ± 3.7 g (8- to 11-month-old mice), indicating that molecular mechanisms involved in age-dependent body weight gain are initiated early in life. We therefore focused the study on those initiating events of obesity in early middle-aged mice rather than in older mice. Throughout this work, 3- to 5-month-old mice are called "young" mice and 8- to 11-month-old mice are termed "aging" mice. We used the term "aging" instead of "aged" or "old" in this context to denote the process of progressively getting older. Age-dependent weight gain was accompanied by a significant increase in the size of adipocytes from epididymal WAT (eWAT) (Figures 1A, 1B, and S1), a visceral WAT depot with a remarkable expansion capacity during aging and a major risk factor for metabolic disease (Rosen and Spiegelman, 2014). To investigate the molecular mechanisms underlying age-dependent WAT enlargement, we focused on mitochondria because of their emerging fundamental role in white adipocyte biology (Bournat and Brown, 2010; Kusminski and Scherer, 2012; Rosen and Spiegelman, 2014; Villarroya et al., 2009) and in aging (López-Otín et al., 2013). Although mitochondrial content of eWAT adipocytes was similar between young and aging mice (Figure 1C), the oxygen consumption rate (OCR) and ATP turnover were significantly lower in eWAT of aging mice (Figures 1D and 1E). More detailed mitochondrial activity analysis revealed a significant decline of CIV activity in aging white adipocytes, whereas complex I, II, I+III, and II+III activities remained unchanged (Figure 1F). Furthermore, western blot analysis showed that the protein levels of representative CIV subunits, such as COX5B, NDUFA4, and mt-CO1, were significantly lower in aging than in young adipocytes (Figures 1G and 1H). By contrast, protein expression levels of NADH dehydrogenase (ubiquinone) 1 alpha subcomplex 9 (NDUFA9; complex I), succinate dehydrogenase complex, subunit A, flavoprotein (Fp) (SDHA; complex II), ubiquinol-cytochrome *c* reductase core protein 1 (UQCRC1; complex III), and mitochondrial voltage-dependent anion channel 1 (VDAC1) were not significantly changed (Figures 1G and 1H). These data show that while mitochondrial oxygen consumption is reduced in aging eWAT, not all mitochondrial complexes are equally affected during this process, and mitochondrial CIV is specifically repressed.

HIF1A Promotes Age-Dependent eWAT Expansion and a Reduction of CIV Expression

To investigate the molecular mechanisms involved in age-dependent regulation of mitochondrial CIV and adipocyte enlargement, we focused on HIF1A because previous studies have demonstrated its activation in aged tissues (Gomes et al., 2013; González-Rodríguez et al., 2012). Although these studies were performed at later stages during the lifespan of the mouse, we wondered whether HIF1A is already expressed in WAT of aging mice (8- to 11-month-old mice). Western blot analysis confirmed that the steady-state levels of HIF1A in eWAT were higher in aging than in young mice (Figure 2A), and this was not seen in other tissues, such as brown adipose tissue or liver (Figure S2A). We therefore questioned whether HIF1A could drive age-dependent white adipocyte enlargement. To do this, we generated mice with global or adipocyte-restricted *Hif1a* gene deficiency using transgenic mice expressing ubiquitin-Cre-ER^{T2} ($Hif1a^{\Delta Ubq}$) or adiponectin-Cre-ER^{T2} ($Hif1a^{\Delta Adipo}$), respectively (Figures S2B and S2F). Aging $Hif1a^{\Delta Ubq}$ and $Hif1a^{\Delta Adipo}$ mice gained significantly less body weight (Figures S2D, S2E, S2G, and S2H) and had smaller eWAT adipocytes (Figures 2B, 2C, and S2C) under normal dietary conditions than aging control mice, suggesting that adipocyte HIF1A drives age-dependent obesity.

Given that HIF1A functions as a transcription factor that can also be involved in gene repression (Eltzschig et al., 2005; Gordan et al., 2007; Krishnan et al., 2012), we next evaluated the possibility that the expression of nuclear-encoded CIV gene transcripts was repressed in aging adipocytes in a HIF1A-dependent manner. By RT-PCR analysis, we found that the levels of *Cox5b*, *Cox6a*, *Cox6c*, and *Cox8a* mRNA were all significantly lower in aging adipocytes than in young adipocytes, whereas the mRNA expression level of other CIV subunits was unaffected (Figure S2I). In addition, only *Cox5b* and *Cox8a* mRNA levels were restored in *Hif1a*-deficient adipocytes (Figure 2D). Only a few CIV genes were

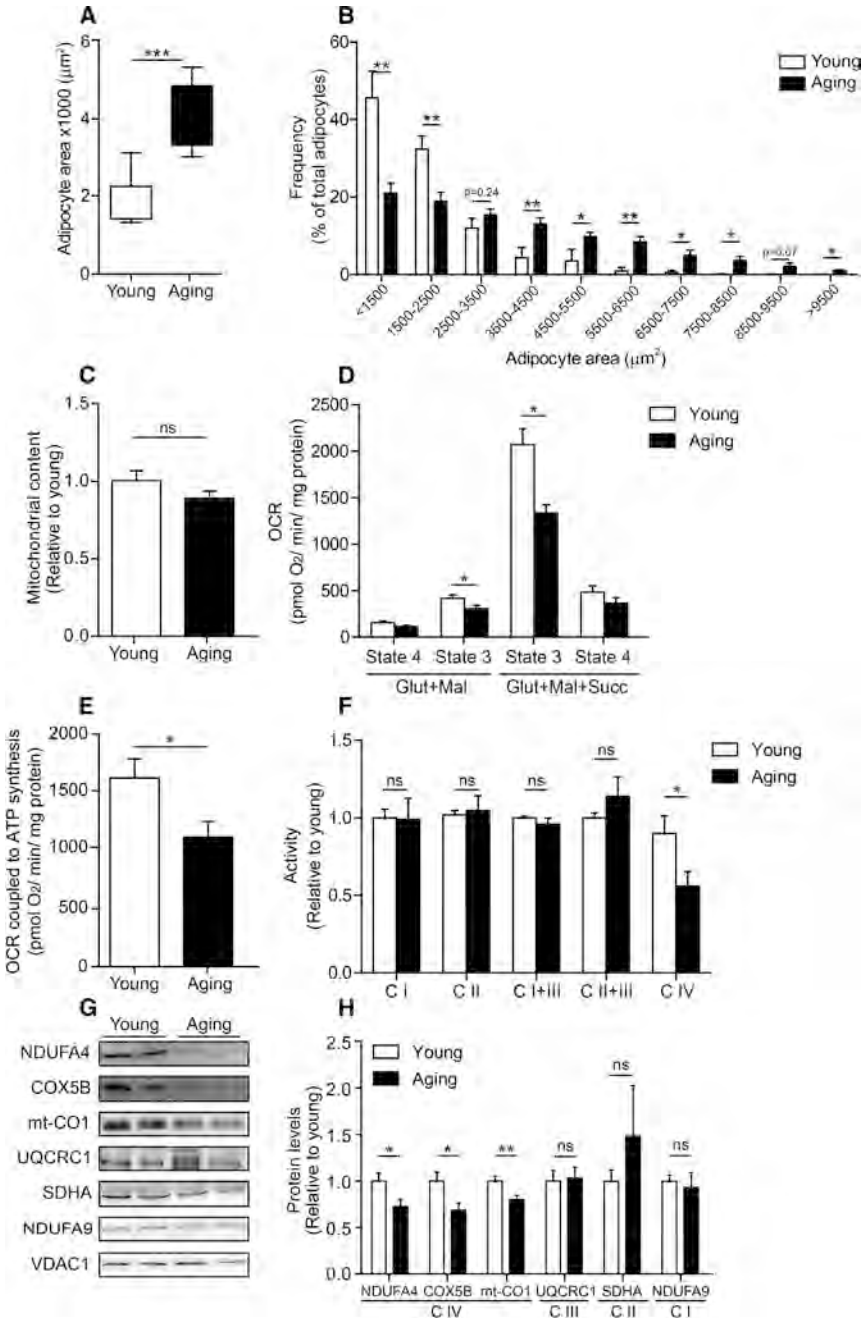

Figure 1. Mitochondrial CIV Activity Is Specifically Decreased during Age-Dependent Obesity in White Adipocytes

(A and B) Average adipocyte area (A) and adipocyte size frequency (B) distribution in young mice (n = 7) and aging mice (n = 5).

(C) Mitochondrial content in isolated white adipocytes of young mice (n = 4) and aging mice (n = 5).

(D) Mitochondrial OCR in eWAT from young mice (n = 6) and aging mice (n = 7). OCR was measured after sequential addition of glutamate and malate (Glut + Mal, State 4), ADP (Glut + Mal, State 3), succinate (Glut + Mal + Succ, State 3), and oligomycin (Glut + Mal + Succ, State 4).

(E) Mitochondrial OCR coupled to ATP synthesis (or ATP turnover) in eWAT from young mice (n = 6) and aging mice (n = 7).

(F) Activities of the indicated mitochondrial ETC complexes were measured in isolated white adipocytes of young mice (n = 6) and aging mice (n = 10).

(G and H) Western blot analysis (G) and quantification of the indicated mitochondrial subunits (H) in isolated white adipocytes of young mice (n = 12) and aging mice (n = 10). Protein expression was normalized to VDAC1.

In bar graphs, values represent mean ± SEM (error bars). In box and whiskers plots, vertical lines connect the minimum and the maximum values. Statistical significance was assessed with a two-tailed t test (*p < 0.05; **p < 0.01; ***p < 0.001; NS, not significant). See also Figure S1.

affected by aging, which was surprising because our analysis of protein content of other representative subunits, such as NDUFA4 or mt-CO1 (Figures 1G and 1H), indicated a more global repression in aging adipocytes. The protein content of NDUFA4 and mt-CO1 was restored by *Hif1a* deletion (Figure 2E), suggesting that HIF1A-dependent repression of *Cox5b* and *Cox8a* mRNAs could lead to reduced protein content of other mitochondrial CIV subunits in aging adipocytes. In this respect, it has been previously shown in a macrophage cell line that *Cox5b* silencing is sufficient to promote global CIV dysfunction by reducing the protein stability of other CIV components (Galati et al., 2009). To test whether COX5B and COX8A control CIV stability in adipocytes, we silenced both in 3T3-L1 cells (Figure 3A) and found reduced protein levels of the mitochondrial CIV subunits NDUFA4 and mt-CO1 (Figure 3B). Moreover, silencing of *Cox5b* resulted in a profound decline of both CIV activity and CIV assembly (Figures 3C and 3D). The ability of COX5B to regulate CIV stability was dose dependent, because silencing *Cox5b* by 90% (as occurred in clone #2) resulted in a stronger inhibition of CIV assembly and activity than that observed when *Cox5b* was reduced by 60%–70% (as occurred in clone #1) (Figures 3C and 3D). In addition, robust silencing of *Cox8a* mRNA (90%–95%) reduced mitochondrial CIV activity and assembly, but to a lesser extent than that observed for *Cox5b* silencing (Figures 3C and 3D). In agreement with these data, CIV assembly was also reduced in aging adipocytes (Figures 3E and 3F).

Collectively, these data show a global decline of CIV in aging white adipocytes that is characterized by repression of CIV activity and assembly. This CIV dysfunction could be initiated by repressing *Cox5b*, as well as *Cox8a*, through HIF1A stabilization during WAT expansion.

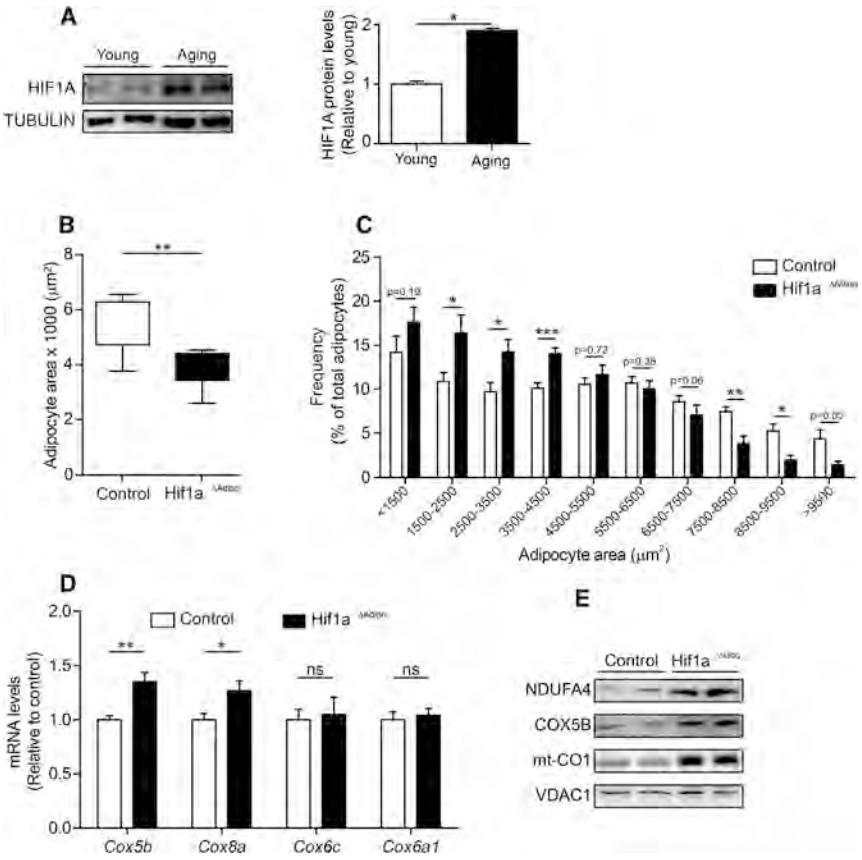

Figure 2. HIF1A Promotes Age-Dependent Complex IV Decline Associated with eWAT Expansion

(A) Representative western blot analysis and quantification of HIF1A in eWAT from young and aging mice.

(B) Average adipocyte size in Hif1a$^{\Delta Adipo}$ mice (n = 6) and *Hif1a*^{floxed} control mice (n = 8) at the age of 8–10 months.

(C) Adipocyte area frequency distribution analysis in Hif1a$^{\Delta Adipo}$ mice (n = 6) and control mice (n = 8) at the age of 8–10 months.

(D) mRNA expression levels of *Cox5b*, *Cox8a*, *Cox6c*, and *Cox6a1* in isolated adipocytes of Hif1a$^{\Delta Adipo}$ mice (n = 6) and *Hif1a*^{floxed} control mice (n = 5) at the age of 8–10 months.

(E) Western blot analysis of CIV subunits (COX5B, NDUFA4, and mt-CO1) in isolated adipocytes of Hif1a$^{\Delta Ubq}$ mice and control mice (control).

In bar graphs, values represent mean ± SEM (error bars). In box and whiskers plots, vertical lines connect the minimum and the maximum values. Statistical significance was assessed with a two-tailed t test (*p < 0.05; **p < 0.01; ***p < 0.001; NS, not significant). See also Figure S2.

HIF1A Binds the *Cox5b* Proximal Promoter

We next examined the molecular link between HIF1A and CIV gene expression, focusing our analysis on *Cox5b* and *Cox8a*. Previous studies have reported a HIF1A-dependent repression of some genes following the binding of HIF1A to their DNA regulatory regions (Eltzschig et al., 2005; Krishnan et al., 2012). We therefore first assessed the presence of HIF1A binding activity in the DNA regulatory regions of *Cox5b* and *Cox8a* (Dhar et al., 2008). Sequence analysis revealed potential HIF1A binding sites from −93 to −97 positions (Figure 4A) and from −760 to −756 positions (Figure S3A) of murine *Cox5b* and *Cox8a* DNA regulatory regions, respectively. Chromatin immunoprecipitation (ChIP) using an anti-HIF1A antibody confirmed the binding of HIF1A to the *Cox5b* proximal promoter region in 3T3-L1 cells exposed to hypoxia (Figure 4B). Moreover, binding of HIF1A was specific to this region, because it was not detected with oligonucleotides directed to amplify a distal region of the *Cox5b* promoter or the *Cox8a* proximal promoter (Figures 4A, 4B, S3A, and S3B). Consistent with HIF1A binding to this region, expression of *Cox5b* mRNA was significantly reduced in 3T3-L1 cells under hypoxia (Figure 4C), whereas the mRNA of the prolyl hydroxylase domain enzyme 3 (*Phd3*), a well-characterized HIF-inducible gene, was increased (Figure S3C). To validate the role of HIF1A in *Cox5b* gene repression, we used *Hif1a*-deficient murine embryonic fibroblasts (MEFs). We first confirmed that repression of *Cox5b* gene expression occurred in wild-type MEF exposed to hypoxia (Figure 4D), whereas *Phd3* expression was elevated (Figure S3D). Moreover, activation of the HIF pathway with dimethyloxaloylglycine (DMOG), a competitive inhibitor of prolyl hydroxylase oxygen sensors, reduced *Cox5b* gene expression in MEF (Figure 4E). As expected, *Cox5b* gene repression by hypoxia or DMOG treatment was markedly attenuated in *Hif1a*-deficient MEF (Figures 4D and 4E), strongly suggesting that HIF1A acts as a transcriptional repressor of *Cox5b*. As a positive control, the expression of *Phd3* was less evident in *Hif1a*-deficient MEF (Figures S3D and S3E).

Overall, these data indicate that *Cox5b* repression is a primary event that occurs upon HIF1A stabilization in aging adipocytes. We therefore further explored the role of CIV in the control of adipocyte size during aging by modifying white adipocyte COX5B expression.

Mitochondrial CIV Inhibition through Silencing of *Cox5b* Promotes Intracellular Lipid Accumulation and White Adipocyte Enlargement

We next determined whether COX5B-dependent mitochondrial CIV repression controls lipid accumulation and age-dependent adipocyte size enlargement. To evaluate intracellular lipid accumulation, 3T3-L1-shCOX5B (small hairpin *COX5B* RNA) cells and control cells were stained with Nile red and intracellular lipids were measured by flow cytometry. Lipid content was higher in 3T3-L1-shCOX5B cells than in control cells (Figures 5A and S4A), suggesting that a reduction in CIV activity by *Cox5b* silencing is sufficient to promote lipid storage. To confirm this finding, 3T3-L1-shSCR (small hairpin scrambled RNA) control cells were treated with sodium azide, a well-established pharmacological inhibitor of CIV. Azide treatment

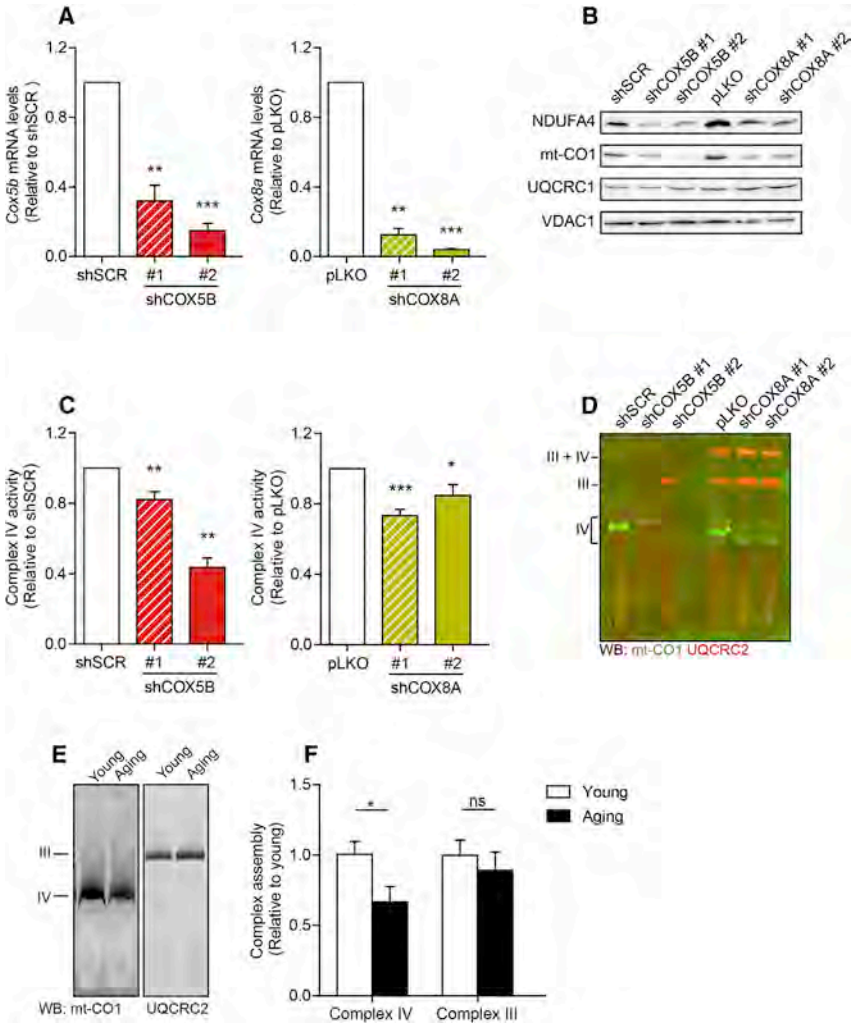

Figure 3. Comparative Analysis of *Cox5b* and *Cox8a* Silencing Effects on CIV Activity and Assembly

(A) Left panel: mRNA expression of *Cox5b* in 3T3-L1-shCOX5B cells using two shRNA sequences: clone 1 (#1) and clone 2 (#2) relative to 3T3-L1-shSCR control cells (n = 4 independent experiments). Right panel: mRNA expression of *Cox8a* in 3T3-L1-shCOX8A cells using two shRNA sequences: clone 1 (#1) and clone 2 (#2) relative to 3T3-L1-pLKO control cells (n = 3 independent experiments).

(B) Western blot analysis of the indicated mitochondrial ETC subunits in 3T3-L1-shCOX5B and 3T3-L1-shCOX8A cells and their respective controls.

(C) CIV activity in 3T3-L1-shCOX5B cells and 3T3-L1-shCOX8A cells and their respective controls.

(D) Blue native-PAGE western blot analysis showing mitochondrial complexes and super-complexes in 3T3-L1-shCOX5B and 3T3-L1-shCOX8A cells and their respective controls. UQCRC2 or mt-CO1 antibody was used to identify complex III or IV assembly.

(E and F) Representative images (E) and quantification (F) of blue native-PAGE analysis of mitochondrial complex III and IV assembly using UQCRC2 or mt-CO1, respectively, in isolated adipocytes of young mice (n = 8) and aging mice (n = 8).

In bar graphs, values represent mean ± SEM (error bars). Statistical significance was assessed with a two-tailed t test (*p < 0.05; **p < 0.01; ***p < 0.001; NS, not significant).

also increased the Nile red signal intensity in 3T3-L1-shSCR control cells (Figure 5A). Because increased fat accumulation has been associated with reduced fatty acid oxidation (Kusminski and Scherer, 2012; Vernochet et al., 2012), we also measured fatty acid oxidation in *Cox5b*-silenced cells. Both 3T3-L1-shCOX5B cells and azide-treated 3T3-L1-shSCR cells presented significantly reduced fatty acid oxidation when compared with control cells (Figure 5B). Furthermore, consistent with aging adipocytes, *Cox5b* silencing in 3T3-L1 cells reduced oxygen consumption and ATP turnover (Figures 5C, 5D, S4B, and S4C). Collectively, these data suggest that repression of *Cox5b* leads to the attenuation of mitochondrial CIV activity, which is sufficient to reduce fatty acid oxidation and promote intracellular lipid accumulation.

We next asked whether *Cox5b* silencing in young mice would promote white adipocyte enlargement in vivo. We therefore injected lentiviral shCOX5B particles into the right eWAT depot of young wild-type mice, while the left contralateral eWAT depot remained uninjected and served as an internal control (Figure 6A). An identical protocol was used for control shSCR particles (Figure 6A). Injection of shCOX5B particles significantly reduced the ratio of *Cox5b* mRNA levels in the injected to non-injected eWAT depot when compared with shSCR mice (Figure 6B), which was concomitant with a significant increase in the adipocyte size ratio (Figure 6C). Moreover, analysis of adipocyte size distribution revealed that shCOX5B-injected eWAT depots contained a greater proportion of large adipocytes and a smaller proportion of small adipocytes than shSCR-injected depots (Figure 6D). No significant differences were found in the contralateral non-injected depots (Figure S5A). Thus, the reduction of COX5B expression in the eWAT of young mice drives white adipocyte enlargement, indicating that *Cox5b* repression is an important determinant of eWAT adipocyte size.

In vivo COX5B Restoration Attenuates Adipocyte Size Enlargement in Aging Mice

These findings prompted us to evaluate whether restoration of COX5B expression could be exploited as a potential molecular target to prevent age-dependent adipocyte enlargement. To do this, we first validated that overexpression of COX5B protein is sufficient to increase mitochondrial CIV activity. Ectopic overexpression of COX5B protein in HEK293T cells (Figure S5B) increased mitochondrial CIV activity (Figure S5C). Next, lentiviral particles overexpressing COX5B were injected into the right eWAT depot of aging mice, while the left contralateral visceral

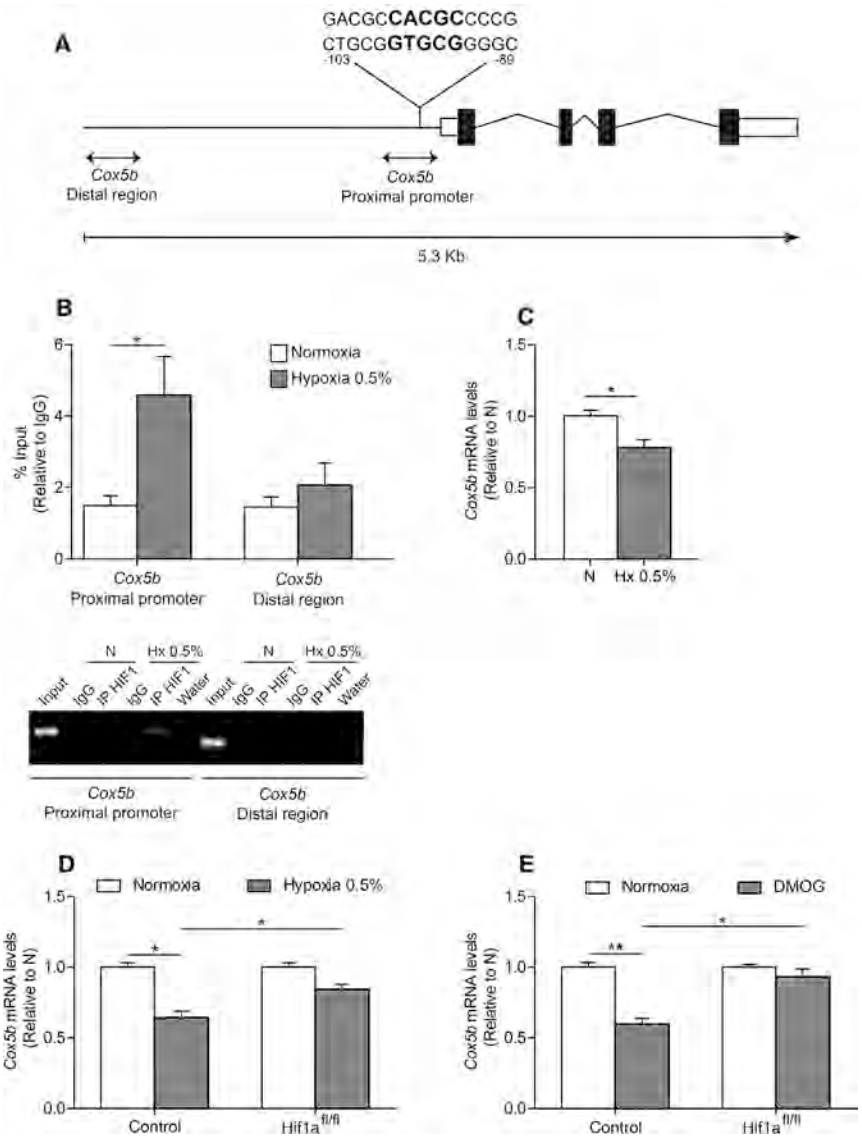

Figure 4. HIF1A Binds to the *Cox5b* Proximal Promoter

(A) Schematic representation of the mouse *Cox5b* gene and its promoter region, indicating the position of the HIF1A binding site in bold.

(B) ChIP assay to assess the relative HIF1A binding activity to the mouse *Cox5b* proximal promoter and distal region in 3T3-L1 cells exposed to normoxia or hypoxia 0.5% for 18–20 hr (n = 7 independent experiments). A representative gel showing DNA amplified in the ChIP assays is shown in the lower panel.

(C) *Cox5b* mRNA expression levels in 3T3-L1 cells exposed to normoxia or hypoxia 0.5% for 72 hr (n = 4 independent experiments).

(D) *Cox5b* mRNA expression levels in control or Hif1a$^{fl/fl}$ MEF exposed to normoxia or hypoxia 0.5% for 48 hr (n = 4 independent experiments).

(E) *Cox5b* mRNA expression levels in control or Hif1a$^{fl/fl}$ MEF under normoxia or 48 hr after 0.5 mM DMOG treatment (n = 4 independent experiments).

In bar graphs, values represent mean ± SEM (error bars). Statistical significance was assessed with a two-tailed t test (*p < 0.05; **p < 0.01). See also Figure S3.

eWAT depot remained uninjected (Figure 6E). An identical protocol was used for control empty vector particles (Figure 6E). Injection of COX5B-expressing lentiviral particles significantly increased the ratio of *Cox5b* mRNA levels in the injected to non-injected eWAT depot when compared with empty vector mice (Figure 6F) and significantly decreased the adipocyte size (Figure 6G). Adipocyte size distribution analysis revealed a greater proportion of small adipocytes and a reduced proportion of large adipocytes in COX5B-injected eWAT depots when compared with the empty vector-injected eWAT depots (Figure 6H), whereas no significant differences were observed in the corresponding non-injected contralateral eWAT depots (Figure S5D).

These in vivo data demonstrate that restoring COX5B expression in visceral eWAT is sufficient to attenuate adipocyte enlargement in aging mice, underscoring the relevance of COX5B to control age-dependent adipocyte size.

Human WAT *COX5B* Expression Correlates Negatively with Age and Serves as a Prognostic Factor for Weight Loss after Bariatric Surgery

Finally, to explore the potential relevance of our findings in humans, we measured *COX5B* expression in human visceral adipose tissue (VAT) during aging in a cohort of subjects with a range of adiposity (anthropometric and clinical parameters are described in the Experimental Procedures section). We found that *COX5B* mRNA levels correlated negatively with age in this cohort (Figure 7A), which persisted after controlling for BMI in multiple linear regression analysis (Figure 7B). Expression of the mitochondrial marker *VDAC1* was not associated with age in this cohort (Figures 7C and 7D), suggesting that the decrease in *COX5B* expression was not attributable to an overall decrease in the expression of mitochondrial components. Thus, the expression of *COX5B* is highly vulnerable to visceral WAT aging, not only in mice but also in human VAT.

We also investigated the clinical value of our findings. Post-bariatric surgery weight reduction shows great disparities among individuals (Lutfi et al., 2006; Maggard et al., 2005), and age has been shown to be a prognostic factor (Scozzari et al., 2012). We therefore asked whether *COX5B* in WAT might predict long-term weight loss in humans after bariatric surgery. We found that subcutaneous white adipose tissue (SAT) *COX5B* levels negatively correlated with BMI 1 year after bariatric surgery (Figure 7E), whereas *VDAC1* showed the opposite trend (Figure 7F). Patients with higher *COX5B* levels had a lower BMI 1 year after bariatric surgery (Figure 7E), underlining the

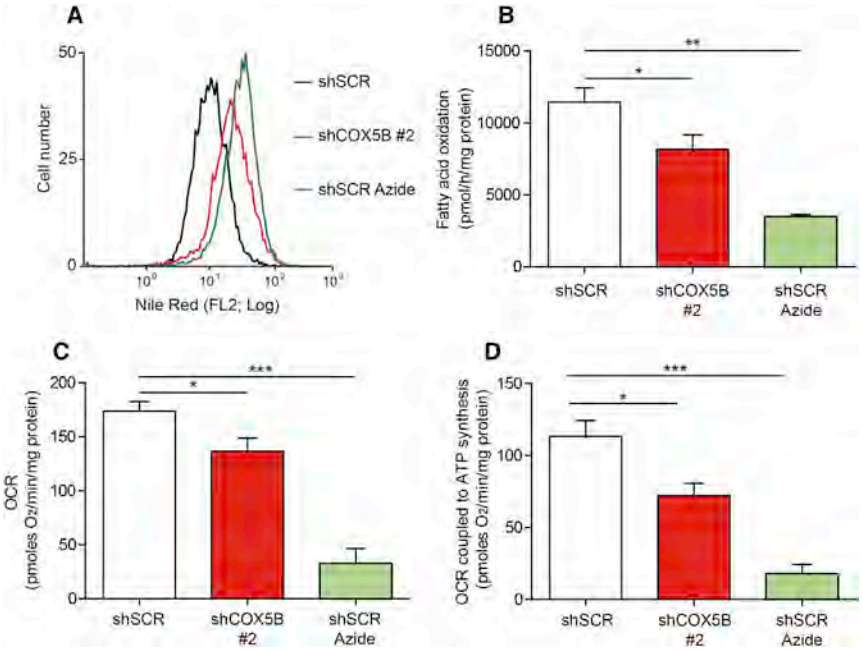

Figure 5. Mitochondrial CIV Inhibition and *Cox5b* Silencing Results in Intracellular Lipid Storage In Vitro and Decreases Mitochondrial Respiration

(A) Nile red fluorescence intensity in 3T3-L1-shCOX5B #2 cells, 3T3-L1-shSCR control cells, and 3T3-L1-shSCR control cells treated with 5 mM azide. A representative experiment out of seven independent experiments is shown.

(B) Fatty acid oxidation in 3T3-L1-shCOX5B #2 cells (n = 6), 3T3-L1-shSCR control cells (n = 5), and 3T3-L1-shSCR control cells treated with 5 mM azide (n = 6).

(C) Mitochondrial OCR in 3T3-L1-shCOX5B #2 cells, 3T3-L1-shSCR control cells, and 3T3-L1-shSCR control cells treated with 5 mM azide (n = 6).

(D) ATP turnover in 3T3-L1-shCOX5B #2 cells, 3T3-L1-shSCR control cells, and 3T3-L1-shSCR control cells treated with 5 mM azide (n = 6).

In bar graphs, values represent mean ± SEM (error bars). Statistical significance was assessed with a two-tailed t test (*p < 0.05; **p < 0.01; ***p < 0.001). See also Figure S4.

translational relevance and clinical value of *COX5B* measurements in SAT. Moreover, SAT samples can be gathered using a minimally invasive biopsy technique (Campbell et al., 2009), which also supports the clinical relevance of measuring *COX5B*.

Overall, our data show that repression of mitochondrial CIV activity is an early sign of age-dependent mitochondrial dysfunction in white adipocytes that drives WAT expansion during aging. Moreover, these data highlight the potential of CIV restoration to prevent increased adipocyte size enlargement during aging.

DISCUSSION

Aging is associated with increased adiposity early in life (Gargiulo et al., 2014; Kuk et al., 2009), suggesting that the molecular mechanisms underlying age-dependent WAT expansion should be initiated at an early stage of the lifetime. This is in contrast to other molecular alterations associated with aging, which are usually studied in very old mice (22- to 30-month-old mice) (Gomes et al., 2013; Houtkooper et al., 2011). Our study shows that mitochondrial CIV activity is specifically compromised in white adipocytes in early phases during aging (8- to 11-month-old mice), although the activity of other mitochondrial complexes, as well as mitochondrial content, are unaltered. Therefore, our study identifies WAT CIV dysfunction as an early sign of aging in white adipocytes that manifests in middle-aged mice, which leads to progressive age-dependent body weight gain during the lifetime.

Previous studies have demonstrated that mitochondrial activity is globally repressed in more severe models of obesity. Accordingly, mice subjected to HFD and mice with altered leptin signaling, such as *ob*/*ob* and *db*/*db* mice, show a significant decline in mitochondrial content in WAT (Choo et al., 2006; Rong et al., 2007; Sutherland et al., 2008; Valerio et al., 2006). It is possible that these settings, which are different from age-dependent obesity, have specific features that provoke global mitochondrial dysfunction in white adipocytes. The reasons for these differences are unclear, but one possible explanation is the excessive nutrient supply in HFD models. Several studies have shown that high levels of nutrients, including free fatty acids, lead to global mitochondrial dysfunction through diverse mechanisms, including oxidative stress and production of inflammatory cytokines (Gao et al., 2010; Kusminski and Scherer, 2012; Sutherland et al., 2008; Valerio et al., 2006). It is therefore conceivable that global mitochondrial dysfunction, including a decrease in mitochondrial content, is a general response to a pathological WAT scenario that is more characterized by nutrient overload. Presumably, this nutrient surplus occurs to a lesser degree, or maybe absent, during age-dependent WAT expansion. Along this line, human studies have shown that mitochondrial content is not consistently repressed in obese subjects (Kaaman et al., 2007; Lindinger et al., 2010; Yin et al., 2014). Lindinger et al. (2010) described a trend for reduced mtDNA content in diabetic obese patients but not in non-diabetic obese patients. In this regard, our present data in human VAT show that the expression of the mitochondrial marker *VDAC1* is not affected during aging, whereas the expression of *COX5B* is significantly repressed, indicating that aging can promote specific mitochondrial alterations in VAT. Furthermore, we show the prognostic potential of *COX5B* measurements in WAT, because patients with higher *COX5B* levels have lower BMI 1 year after bariatric surgery. These data are in accordance with a study showing that younger patients experienced a significantly greater and prolonged BMI decrease after surgery (Scozzari et al., 2012).

Previous studies have detected hypoxia in WAT under normal dietary conditions, based on pimonidazole staining (Hosogai et al., 2007; Lee et al., 2011; Ye et al., 2007). These data might explain the basal HIF1A expression observed in WAT of young mice (Figure 2A) (Krishnan et al., 2012; Lee et al., 2014; Yin

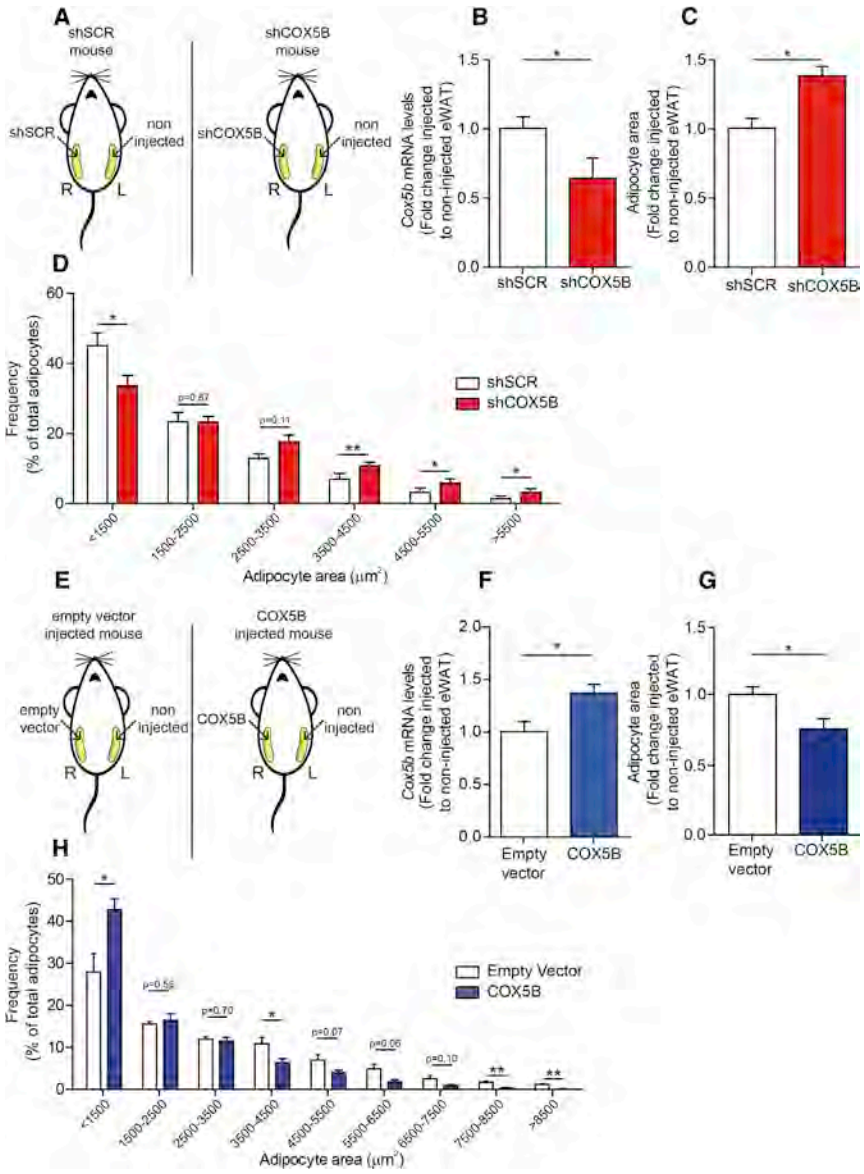

Figure 6. Opposing Effects of In Vivo Silencing and Restoration of *Cox5b* Expression in eWAT

(A) Schematic representation of eWAT injection of shSCR and shCOX5B lentiviral particles in mice.

(B) Ratio of *Cox5b* mRNA expression levels in injected to non-injected eWAT depots of shCOX5B mice (n = 4) and shSCR mice (n = 4). Fold change relative to shSCR is shown.

(C) Ratio of average adipocyte size in injected to non-injected eWAT depot of shCOX5B mice (n = 4) and shSCR mice (n = 4). Fold change relative to shSCR is shown.

(D) Adipocyte area frequency distribution analysis in shCOX5B (n = 4) and shSCR (n = 4) injected depots.

(E) Schematic representation of eWAT injection of COX5B and empty vector lentiviral particles in mice.

(F) Ratio of *Cox5b* mRNA expression in injected to non-injected eWAT depot of COX5B mice (n = 4) and empty vector mice (n = 5). Fold change relative to empty vector is shown.

(G) Ratio of average adipocyte size in injected to non-injected eWAT depots of COX5B mice (n = 4) and empty vector mice (n = 4). Fold change relative to empty vector is shown.

(H) Adipocyte area frequency distribution analysis in COX5B (n = 4) and empty vector (n = 4) injected depots.

In bar graphs, values represent mean ± SEM (error bars). Statistical significance was assessed with a two-tailed t test (*$p < 0.05$; **$p < 0.01$). See also Figure S5.

et al., 2009), which drives CIV repression and subsequent fat accumulation during aging. This latter contention is in line with a previous study showing that adipocyte-restricted inactivation of *Arnt*, a transcription factor with multiple partners, including HIF1A, counteracts age-dependent body weight gain (Lee et al., 2011). In addition, adipocyte-restricted *Hif1a* gene inactivation counteracts pathological WAT expansion in HFD-fed mice (Jiang et al., 2011; Krishnan et al., 2012; Lee et al., 2011, 2014). Regarding the molecular mechanisms executed by HIF1A leading to age-dependent white adipocyte enlargement, we found that HIF1A represses *Cox5b* and *Cox8a* gene expression. Previous studies have reported HIF1A-dependent gene repression associated with the binding of HIF1A to DNA regulatory regions of target genes (Eltzschig et al., 2005; Krishnan et al., 2012). In the present study, we found that hypoxia induces HIF1A binding to the *Cox5b* proximal promoter, which was associated with *Cox5b* repression. This promoter region has been previously shown to sustain *Cox5b* gene expression through NRF1 transcription factors (Dhar et al., 2008), suggesting that HIF1A could interfere with its basal activity. By contrast, although we acknowledge that HIF1A-dependent *Cox8a* repression can potentially cooperate with *Cox5b* to reduce CIV activity in aging adipocytes, we did not find HIF1A binding activity at the *Cox8a* proximal promoter, suggesting that HIF1A could drive *Cox8a* repression by indirect mechanisms, as described for other target genes repressed by HIF1A (Chan et al., 2009). Our analysis also shows that *Cox6a* and *Cox6c* expression in white adipocytes declined during age-dependent body weight gain but was not restored upon *Hif1a* deletion in aging adipocytes, suggesting that their regulation is executed by other hypoxia-dependent pathways (Sena and Chandel, 2012) or as a consequence of fat accumulation (Lee et al., 2014). A previous study has shown that HIF1A induces a COX4.2/COX4.1 switch to protect cells against hypoxia-induced reactive oxygen species (ROS) by optimizing respiration efficiency (Fukuda et al., 2007). However, we have not found evidence of this metabolic adaptation in aging WAT, suggesting that perhaps this switch is not operative in white adipocytes or

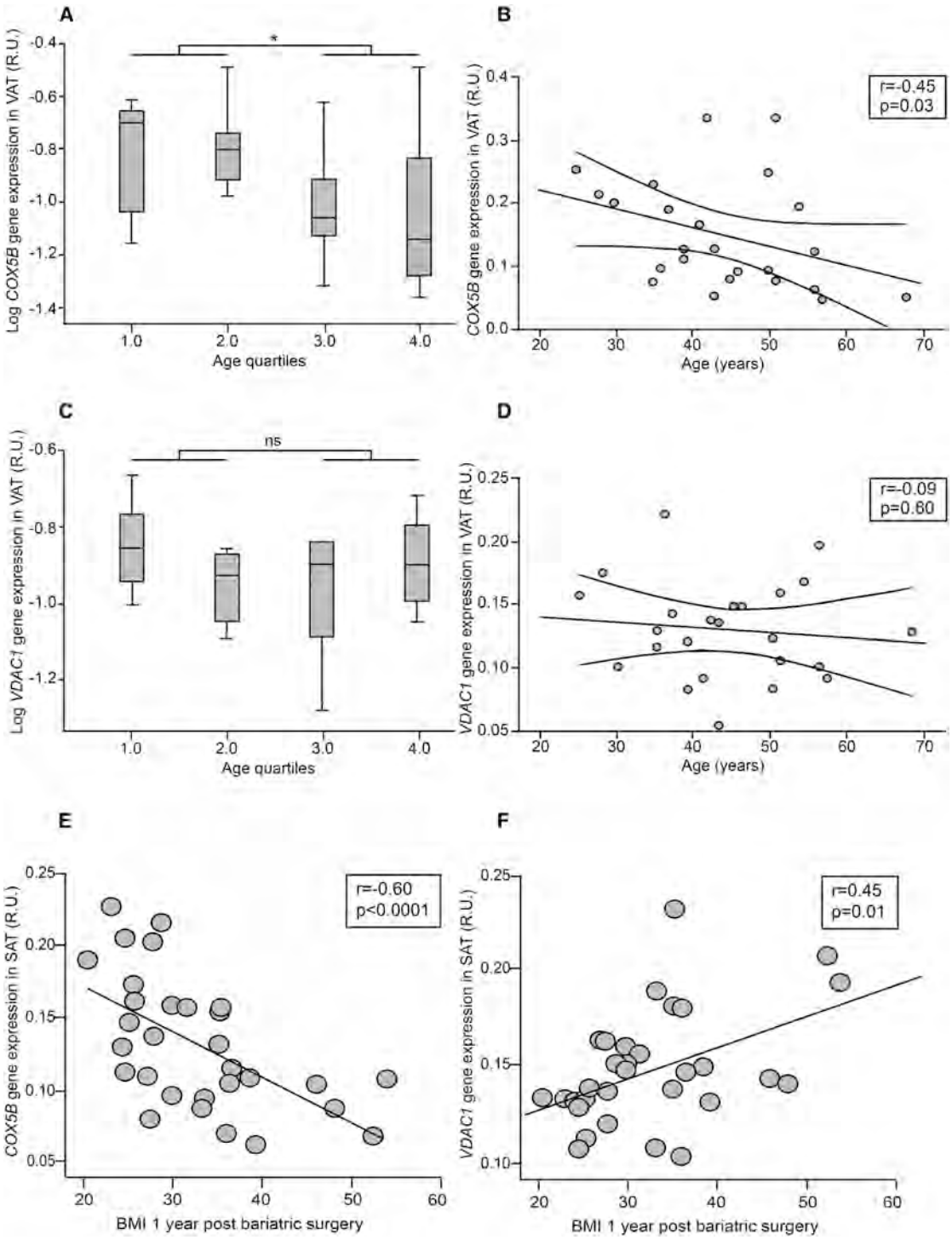

Figure 7. Age-Dependent Repression of *COX5B* Gene Expression in Human VAT and *COX5B* as a Prognostic Factor in Bariatric Surgery

(A–D) Boxplots showing log *COX5B* (A) or VDAC (C) gene expression in human VAT with increasing age quartiles (see Experimental Procedures); vertical lines connect the minimum and the maximum values (n = 24). Linear correlation analysis of the association between *COX5B* (B) or VDAC (D) gene expression in human VAT and age. Results remained significant after adjusting for Deuremberg-calculated fat mass instead of BMI.

(E and F) Linear correlation analysis of the association between *COX5B* (E) or VDAC (F) gene expression in human subcutaneous white adipose tissue (SAT) and BMI 1 year after bariatric surgery (n = 31).

Differences in human gene expression across age quartiles were evaluated with one-way ANOVA (*$p < 0.05$; NS, not significant). Linear association between gene expression and age or BMI was evaluated with Spearman's rank test.

it requires a more robust activation of HIF1A than that observed in aging adipocytes in vivo. Collectively, our data suggest that HIF1A-dependent repression of *Cox5b* expression can be considered a primary event, leading to a more global CIV decline because of the central role of COX5B in CIV stability, and further establish a molecular link between HIF1A and CIV, wherein HIF1A acts as a global repressor of CIV expression in white adipocytes.

Adipocyte-restricted inactivation and overexpression of key genes involved in mitochondrial biogenesis and activity is fundamental to better understand the role of mitochondria in adipocyte biology. It has been hypothesized that inactivation of these genes would reduce mitochondrial activity, leading to intracellular accumulation of lipids that cannot be oxidized (Kusminski et al., 2012; Vernochet et al., 2012, 2014). For example, reduced adipocyte mitochondrial activity and increased adipocyte size was detected in mice with adipose tissue-restricted overexpression of mitoNEET, an iron-sulfur protein that inhibits mitochondrial iron transport into the matrix and lowers the rate of β-oxidation (Kusminski et al., 2012). However, other studies have shown that adipocyte-restricted inactivation of the mitochondrial transcription factor A (TFAM), which is essential for maintenance of mtDNA, does not lead to increased adiposity because of an unanticipated compensatory response leading to increased mitochondrial oxygen consumption and uncoupling (Vernochet et al., 2012). Moreover, a second mouse model in which *Tfam* was inactivated in adipose tissue to a greater extent revealed a profound and global dysfunction of mitochondria, resulting in adipocyte death and subsequent lipodystrophy (Vernochet et al., 2014). In contrast to these studies, our data indicate that mitochondrial CIV dysfunction through *Cox5b* repression is sufficient to drive intracellular lipid accumulation. Our data suggest that a decline in COX5B protein content cannot be followed by compensatory mitochondrial overactivation or adipocyte death and culminates in enhanced adipocyte lipid content. Therefore, it is possible that during age-dependent body weight gain, repression of *Cox5b* guarantees enhanced lipid storage without these secondary compensatory effects on mitochondrial activity or adipocyte death.

In summary, our data establish mitochondrial CIV, and particularly COX5B, as a vulnerable mitochondrial component during visceral WAT aging in mice and humans. *Cox5b* repression is mediated by the HIF1A pathway and is sufficient to promote age-dependent white adipocyte enlargement. Moreover, our findings highlight the potential of COX5B restoration in visceral WAT to counteract age-dependent adipocyte expansion.

EXPERIMENTAL PROCEDURES

White Adipocyte Isolation

Epididymal fat pads were removed, minced, and digested using collagenase type II (Calbiochem) at 37°C for 1 hr in Krebs-Ringer-HEPES-bicarbonate (KRH) buffer supplemented with BSA (3.5%; Roche). The digested tissue was filtered through a 100 μm cell strainer (BD Falcon), and the floating adipocytes were recovered and used for RNA or protein extraction.

Mitochondrial Content

Relative concentrations of nuclear DNA and mtDNA were determined by RT-PCR. In brief, DNA was isolated from adipocytes using UltraPure phenol: chlorofom:isoamyl alcohol (25:24:1; Invitrogen) after proteinase K (Ambion) digestion at 56°C overnight. Nuclear DNA and mtDNA were measured using a Power SYBR Green PCR Master Mix kit (Applied Biosystems). The amplification data were analyzed using StepOne Software v.2.0 (Applied Biosystems). The following primer sets were used: Genomic *Hprt*: forward 5′-TGGGAGGC CATCACATTGT-3′; reverse 5′-TCCAGCAGGTCAGCAAAGAA-3′. Genomic *mt-Co1*: forward 5′-GCTAGCCGCAGGCATTACTATAC-3′; reverse 5′-GCG GGATCAAAGAAAGTTGTG-3′.

Viral Injection In Vivo

Mice were anesthetized by isoflurane (Abbott) before dissection of the skin and body wall. The lentiviral preparation ($1 \times 10^{7-8}$ plaque-forming units in a volume of 100 μl) was injected into the right eWAT depot distributed in four to six injections of 20–25 μl (each mouse was injected with 100–150 μl of lentiviral preparation). The left contralateral eWAT depot remained uninjected and served as an internal control. Separate mice were injected with different lentiviral particles. Mice injected with virus containing small hairpin RNA (shRNA) against *Cox5b* were sacrificed 2–3 weeks after surgery, and the tissues of interest were removed. Mice injected with virus containing overexpressing COX5B were sacrificed 5–6 weeks after surgery, and the tissues of interest were removed. Mice were randomly allocated to the treatment groups (shSCR group versus shCOX5B group, as well as empty vector group versus COX5B group).

Histological Analysis

Adipose tissue from eWAT depots was isolated and fixed for at least 24 hr in 4%–10% formaldehyde before embedding in paraffin. Sections (5–7 μm; Leica RM2135 microtome) were subjected to standard H&E staining and analyzed using CellD Olympus software (Olympus). At least 200 adipocytes per mouse were analyzed for adipocyte surface area measurement. For adipocyte size quantification in eWAT of injected or non-injected mice, $Hif1a^{\Delta Adipo}$ or control mice, and young or aging mice, the investigator was blinded to the group allocation.

Statistical Analysis

Data are expressed as mean ± SEM (error bars). In box and whiskers plots, vertical lines connect the minimum and the maximum values. All statistical analyses were performed using GraphPad Prism software, and differences between groups with similar variances were analyzed with a two-tailed t test. When variances of the groups were significantly different, a two-tailed t test with Welch's correction was used. Differences between variances of the groups were analyzed with the Fisher test (F-test). A p value lower than 0.05 was considered significant: $^{*}p < 0.05$, $^{**}p < 0.01$, and $^{***}p < 0.001$. Differences in human gene expression factors across age quartiles were evaluated using one-way ANOVA. Linear association between gene expression factors and age was evaluated using Spearman's rank test. A multiple linear regression analysis in a stepwise procedure was used to adjust for BMI. Deuremberg-calculated fat mass was evaluated using the following formula: percent fat mass = 1.2 × (BMI) + 0.23 × (age (years)) − 10.8 × (sex) − 5.4, where sex = 0 in women and sex = 1 in men.

Ethics Statement

All animal experimental procedures were approved by the Research Ethics Committee at the Autonomous University of Madrid (UAM). Experiments were carried out under the supervision of the head of animal welfare and health at the UAM and in accordance with Spanish and European guidelines (RD 53/2013; B.O.E, February 1, 2013). Regarding human data, all subjects gave written informed consent after the purpose of the study was explained to them, and the study was approved by the Ethics Committee of the Hospital of Girona.

SUPPLEMENTAL INFORMATION

Supplemental Information includes Supplemental Experimental Procedures and five figures and can be found with this article online at http://dx.doi.org/10.1016/j.celrep.2016.08.041.

AUTHOR CONTRIBUTIONS

I.S.-A. and Q.O.Y.L. conducted most of the experiments. I.S.-A., Q.O.Y.L., K.D.B., and J.A. were involved in the design of the experiments, data analysis, and writing the manuscript. M.T.-C. helped with histological analysis of WAT paraffin sections. A.E., D.T., and E.F. helped with western blotting and gene expression analysis. E.R. and E.B. helped with metabolic measurements. S.V. and A.Z. helped with histological analysis of WAT paraffin sections in global *Hif1a*-deficient mice. F.M.-R. helped with ChIP experiments. D.S. and A.Z. helped with in vivo oxygen consumption experiments. J.A.E., S.C., P.H.-A., and A.M.-R. helped with Blue-Native PAGE experiments. P.H.-A. and A.M.-R. helped with in vitro oxygen consumption experiments. E.F. helped with intracellular lipid accumulation experiments. K.D.B. and K.V. helped with fatty acid oxidation measurements. J.M.M.-N. and J.M.F.-R. helped with gene expression analysis in human WAT samples.

ACKNOWLEDGMENTS

The authors thank Dr. Francisco Sanchez-Madrid, Dr. Manuel O. de Landázuri, Dr. Luis del Peso, Dr. Victor Javier Sanchez-Arevalo, Dr. Barbara Acosta, and Dr. Maria Tiana for scientific advice and critical reading of the manuscript. We also thank Dr. Stefan Offermanns (Max-Planck Institute for Heart and Lung Research) and Prof. Pierre Chambon (GIE-CERB) for helping us to obtain the adipoq-CreERT2 mice. This work was supported by grants from the Ministerio de Educación y Ciencia (SAF2011-29716 and SAF2013-46058-R), Red de Cardiovascular (RD12/0042/0065), CICYT (SAF2007-60592), CAM (P2010/BMD-2542), and the European Commission (ref. 282551).

Received: June 1, 2015
Revised: September 14, 2015
Accepted: August 14, 2016
Published: September 13, 2016

REFERENCES

Bournat, J.C., and Brown, C.W. (2010). Mitochondrial dysfunction in obesity. Curr. Opin. Endocrinol. Diabetes Obes. *17*, 446–452.

Campbell, K.L., Makar, K.W., Kratz, M., Foster-Schubert, K.E., McTiernan, A., and Ulrich, C.M. (2009). A pilot study of sampling subcutaneous adipose tissue to examine biomarkers of cancer risk. Cancer Prev. Res. (Phila.) *2*, 37–42.

Chan, S.Y., Zhang, Y.Y., Hemann, C., Mahoney, C.E., Zweier, J.L., and Loscalzo, J. (2009). MicroRNA-210 controls mitochondrial metabolism during hypoxia by repressing the iron-sulfur cluster assembly proteins ISCU1/2. Cell Metab. *10*, 273–284.

Choo, H.J., Kim, J.H., Kwon, O.B., Lee, C.S., Mun, J.Y., Han, S.S., Yoon, Y.S., Yoon, G., Choi, K.M., and Ko, Y.G. (2006). Mitochondria are impaired in the adipocytes of type 2 diabetic mice. Diabetologia *49*, 784–791.

Dhar, S.S., Ongwijitwat, S., and Wong-Riley, M.T. (2008). Nuclear respiratory factor 1 regulates all ten nuclear-encoded subunits of cytochrome *c* oxidase in neurons. J. Biol. Chem. *283*, 3120–3129.

Eltzschig, H.K., Abdulla, P., Hoffman, E., Hamilton, K.E., Daniels, D., Schönfeld, C., Löffler, M., Reyes, G., Duszenko, M., Karhausen, J., et al. (2005). HIF-1-dependent repression of equilibrative nucleoside transporter (ENT) in hypoxia. J. Exp. Med. *202*, 1493–1505.

Fukuda, R., Zhang, H., Kim, J.W., Shimoda, L., Dang, C.V., and Semenza, G.L. (2007). HIF-1 regulates cytochrome oxidase subunits to optimize efficiency of respiration in hypoxic cells. Cell *129*, 111–122.

Galati, D., Srinivasan, S., Raza, H., Prabu, S.K., Hardy, M., Chandran, K., Lopez, M., Kalyanaraman, B., and Avadhani, N.G. (2009). Role of nuclear-encoded subunit Vb in the assembly and stability of cytochrome *c* oxidase complex: implications in mitochondrial dysfunction and ROS production. Biochem. J. *420*, 439–449.

Gao, C.L., Zhu, C., Zhao, Y.P., Chen, X.H., Ji, C.B., Zhang, C.M., Zhu, J.G., Xia, Z.K., Tong, M.L., and Guo, X.R. (2010). Mitochondrial dysfunction is induced by high levels of glucose and free fatty acids in 3T3-L1 adipocytes. Mol. Cell. Endocrinol. *320*, 25–33.

Gargiulo, S., Gramanzini, M., Megna, R., Greco, A., Albanese, S., Manfredi, C., and Brunetti, A. (2014). Evaluation of growth patterns and body composition in C57Bl/6J mice using dual energy X-ray absorptiometry. BioMed Res. Int. *2014*, 253067.

Gomes, A.P., Price, N.L., Ling, A.J., Moslehi, J.J., Montgomery, M.K., Rajman, L., White, J.P., Teodoro, J.S., Wrann, C.D., Hubbard, B.P., et al. (2013). Declining NAD(+) induces a pseudohypoxic state disrupting nuclear-mitochondrial communication during aging. Cell *155*, 1624–1638.

González-Rodríguez, A., Más-Gutierrez, J.A., Mirasierra, M., Fernandez-Pérez, A., Lee, Y.J., Ko, H.J., Kim, J.K., Romanos, E., Carrascosa, J.M., Ros, M., et al. (2012). Essential role of protein tyrosine phosphatase 1B in obesity-induced inflammation and peripheral insulin resistance during aging. Aging Cell *11*, 284–296.

Gordan, J.D., Bertout, J.A., Hu, C.J., Diehl, J.A., and Simon, M.C. (2007). HIF-2alpha promotes hypoxic cell proliferation by enhancing c-myc transcriptional activity. Cancer Cell *11*, 335–347.

Hosogai, N., Fukuhara, A., Oshima, K., Miyata, Y., Tanaka, S., Segawa, K., Furukawa, S., Tochino, Y., Komuro, R., Matsuda, M., and Shimomura, I. (2007). Adipose tissue hypoxia in obesity and its impact on adipocytokine dysregulation. Diabetes *56*, 901–911.

Houtkooper, R.H., Argmann, C., Houten, S.M., Cantó, C., Jeninga, E.H., Andreux, P.A., Thomas, C., Doenlen, R., Schoonjans, K., and Auwerx, J. (2011). The metabolic footprint of aging in mice. Sci. Rep. *1*, 134.

Jiang, C., Qu, A., Matsubara, T., Chanturiya, T., Jou, W., Gavrilova, O., Shah, Y.M., and Gonzalez, F.J. (2011). Disruption of hypoxia-inducible factor 1 in adipocytes improves insulin sensitivity and decreases adiposity in high-fat diet-fed mice. Diabetes *60*, 2484–2495.

Kaaman, M., Sparks, L.M., van Harmelen, V., Smith, S.R., Sjölin, E., Dahlman, I., and Arner, P. (2007). Strong association between mitochondrial DNA copy number and lipogenesis in human white adipose tissue. Diabetologia *50*, 2526–2533.

Kim, J.Y., van de Wall, E., Laplante, M., Azzara, A., Trujillo, M.E., Hofmann, S.M., Schraw, T., Durand, J.L., Li, H., Li, G., et al. (2007). Obesity-associated improvements in metabolic profile through expansion of adipose tissue. J. Clin. Invest. *117*, 2621–2637.

Koh, E.H., Park, J.Y., Park, H.S., Jeon, M.J., Ryu, J.W., Kim, M., Kim, S.Y., Kim, M.S., Kim, S.W., Park, I.S., et al. (2007). Essential role of mitochondrial function in adiponectin synthesis in adipocytes. Diabetes *56*, 2973–2981.

Krishnan, J., Danzer, C., Simka, T., Ukropec, J., Walter, K.M., Kumpf, S., Mirtschink, P., Ukropcova, B., Gasperikova, D., Pedrazzini, T., and Krek, W. (2012). Dietary obesity-associated Hif1α activation in adipocytes restricts fatty acid oxidation and energy expenditure via suppression of the Sirt2-NAD+ system. Genes Dev. *26*, 259–270.

Kuk, J.L., Saunders, T.J., Davidson, L.E., and Ross, R. (2009). Age-related changes in total and regional fat distribution. Ageing Res. Rev. *8*, 339–348.

Kusminski, C.M., and Scherer, P.E. (2012). Mitochondrial dysfunction in white adipose tissue. Trends Endocrinol. Metab. *23*, 435–443.

Kusminski, C.M., Holland, W.L., Sun, K., Park, J., Spurgin, S.B., Lin, Y., Askew, G.R., Simcox, J.A., McClain, D.A., Li, C., and Scherer, P.E. (2012). MitoNEET-driven alterations in adipocyte mitochondrial activity reveal a crucial adaptive process that preserves insulin sensitivity in obesity. Nat. Med. *18*, 1539–1549.

Lee, K.Y., Gesta, S., Boucher, J., Wang, X.L., and Kahn, C.R. (2011). The differential role of Hif1β/Arnt and the hypoxic response in adipose function, fibrosis, and inflammation. Cell Metab. *14*, 491–503.

Lee, Y.S., Kim, J.W., Osborne, O., Oh, D.Y., Sasik, R., Schenk, S., Chen, A., Chung, H., Murphy, A., Watkins, S.M., et al. (2014). Increased adipocyte O2 consumption triggers HIF-1α, causing inflammation and insulin resistance in obesity. Cell *157*, 1339–1352.

Lindinger, A., Peterli, R., Peters, T., Kern, B., von Flüe, M., Calame, M., Hoch, M., Eberle, A.N., and Lindinger, P.W. (2010). Mitochondrial DNA content in human omental adipose tissue. Obes. Surg. *20*, 84–92.

López-Otín, C., Blasco, M.A., Partridge, L., Serrano, M., and Kroemer, G. (2013). The hallmarks of aging. Cell *153*, 1194–1217.

Lutfi, R., Torquati, A., Sekhar, N., and Richards, W.O. (2006). Predictors of success after laparoscopic gastric bypass: a multivariate analysis of socioeconomic factors. Surg. Endosc. *20*, 864–867.

Maggard, M.A., Shugarman, L.R., Suttorp, M., Maglione, M., Sugerman, H.J., Livingston, E.H., Nguyen, N.T., Li, Z., Mojica, W.A., Hilton, L., et al. (2005). Meta-analysis: surgical treatment of obesity. Ann. Intern. Med. *142*, 547–559.

Ng, M., Fleming, T., Robinson, M., Thomson, B., Graetz, N., Margono, C., Mullany, E.C., Biryukov, S., Abbafati, C., Abera, S.F., et al. (2014). Global, regional, and national prevalence of overweight and obesity in children and adults during 1980–2013: a systematic analysis for the Global Burden of Disease Study 2013. Lancet *384*, 766–781.

Ogden, C.L., Carroll, M.D., Kit, B.K., and Flegal, K.M. (2013). Prevalence of obesity among adults: United States, 2011–2012. NCHS Data Brief *131*, 1–8.

Rong, J.X., Qiu, Y., Hansen, M.K., Zhu, L., Zhang, V., Xie, M., Okamoto, Y., Mattie, M.D., Higashiyama, H., Asano, S., et al. (2007). Adipose mitochondrial biogenesis is suppressed in db/db and high-fat diet-fed mice and improved by rosiglitazone. Diabetes *56*, 1751–1760.

Rosen, E.D., and Spiegelman, B.M. (2014). What we talk about when we talk about fat. Cell *156*, 20–44.

Saraste, M. (1999). Oxidative phosphorylation at the fin de siècle. Science *283*, 1488–1493.

Scozzari, G., Passera, R., Benvenga, R., Toppino, M., and Morino, M. (2012). Age as a long-term prognostic factor in bariatric surgery. Ann. Surg. *256*, 724–728, discussion 728–729.

Sena, L.A., and Chandel, N.S. (2012). Physiological roles of mitochondrial reactive oxygen species. Mol. Cell *48*, 158–167.

Sutherland, L.N., Capozzi, L.C., Turchinsky, N.J., Bell, R.C., and Wright, D.C. (2008). Time course of high-fat diet-induced reductions in adipose tissue mitochondrial proteins: potential mechanisms and the relationship to glucose intolerance. Am. J. Physiol. Endocrinol. Metab. *295*, E1076–E1083.

Valerio, A., Cardile, A., Cozzi, V., Bracale, R., Tedesco, L., Pisconti, A., Palomba, L., Cantoni, O., Clementi, E., Moncada, S., et al. (2006). TNF-alpha downregulates eNOS expression and mitochondrial biogenesis in fat and muscle of obese rodents. J. Clin. Invest. *116*, 2791–2798.

van Harmelen, V., Skurk, T., Röhrig, K., Lee, Y.M., Halbleib, M., Aprath-Husmann, I., and Hauner, H. (2003). Effect of BMI and age on adipose tissue cellularity and differentiation capacity in women. Int. J. Obes. Relat. Metab. Disord. *27*, 889–895.

Vernochet, C., Mourier, A., Bezy, O., Macotela, Y., Boucher, J., Rardin, M.J., An, D., Lee, K.Y., Ilkayeva, O.R., Zingaretti, C.M., et al. (2012). Adipose-specific deletion of TFAM increases mitochondrial oxidation and protects mice against obesity and insulin resistance. Cell Metab. *16*, 765–776.

Vernochet, C., Damilano, F., Mourier, A., Bezy, O., Mori, M.A., Smyth, G., Rosenzweig, A., Larsson, N.G., and Kahn, C.R. (2014). Adipose tissue mitochondrial dysfunction triggers a lipodystrophic syndrome with insulin resistance, hepatosteatosis, and cardiovascular complications. FASEB J. *28*, 4408–4419.

Villarroya, J., Giralt, M., and Villarroya, F. (2009). Mitochondrial DNA: an up-and-coming actor in white adipose tissue pathophysiology. Obesity (Silver Spring) *17*, 1814–1820.

Yang, S.B., Tien, A.C., Boddupalli, G., Xu, A.W., Jan, Y.N., and Jan, L.Y. (2012). Rapamycin ameliorates age-dependent obesity associated with increased mTOR signaling in hypothalamic POMC neurons. Neuron *75*, 425–436.

Ye, J., Gao, Z., Yin, J., and He, Q. (2007). Hypoxia is a potential risk factor for chronic inflammation and adiponectin reduction in adipose tissue of ob/ob and dietary obese mice. Am. J. Physiol. Endocrinol. Metab. *293*, E1118–E1128.

Yin, J., Gao, Z., He, Q., Zhou, D., Guo, Z., and Ye, J. (2009). Role of hypoxia in obesity-induced disorders of glucose and lipid metabolism in adipose tissue. Am. J. Physiol. Endocrinol. Metab. *296*, E333–E342.

Yin, X., Lanza, I.R., Swain, J.M., Sarr, M.G., Nair, K.S., and Jensen, M.D. (2014). Adipocyte mitochondrial function is reduced in human obesity independent of fat cell size. J. Clin. Endocrinol. Metab. *99*, E209–E216.